Enhancement of Neel Relaxation at Magnetic Heating Performance of Iron Oxide Nanoparticles

Musa Can (musa.can@istanbul.edu.tr)
Renewable Energy and Oxide Hybrid Systems Laboratory, Department of Physics, Faculty of Science, Istanbul University, Istanbul, Turkey

Chasan Bairam
Istanbul University

Seda Aksoy
Istanbul Technical University

Serap Kuruca
Istanbul University

Zerrin Aktaş
Istanbul University

Mustafa Öncül
Istanbul University

Research Article

Keywords: oxide semiconductor, point defects, Neel relaxation, magnetic hypertermia, superparamagnetic nanoparticles

Posted Date: January 23rd, 2021

DOI: https://doi.org/10.21203/rs.3.rs-149474/v1

Enhancement of Neel Relaxation at Magnetic Heating Performance of Iron Oxide Nanoparticles

Musa Mutlu Can[1,*], Chasan Bairam[1], Seda Aksoy[2], Dürdane Serap Kuruca[3], Zerrin Aktaş[4], Mustafa Oral Öncül[5]

[1]Renewable Energy and Oxide Hybrid Systems Laboratory, Department of Physics, Faculty of Science, Istanbul University, Istanbul, Turkey

[2] Department of Physics Engineering, Istanbul Technical University, 34469, Maslak, Istanbul, Turkey

[3]Department of Physiology, Faculty of Medicine, Istanbul University, Istanbul, Turkey

[4]Faculty of Medicine, Department of Clinical Microbiology, Istanbul University, Istanbul, Turkey

[5]Faculty of Medicine, Department of Infectious Diseases and Clinical Microbiology, Istanbul University, Istanbul, Turkey

Abstract

The study is based on understand the titanium (Ti) doping effect to enhance the Neel relaxation at magnetic heating performance of magnetite (Fe_3O_4). Ti doped magnetite ($(Fe_{1-x},Ti_x)_3O_4$; x= 0.02, 0.03 and 0.05) superparamagnetic nanoparticles were synthesized via sol-gel technique. The analyses were performed for $(Fe_{1-x},Ti_x)_3O_4$ and core-shell (SiO_2 coated $(Fe_{1-x},Ti_x)_3O_4$) nanoparticles in order to understand the influence of silica coating on the magnetic properties of nanoparticles. The target of study to enhance the Neel relaxation mechanism on magnetic heating. The interparticle spacing and Ti amount were two parameters that we focused on the study. The results provided that coating with SiO_2 has no specific effect on heating performance of $(Fe_{1-x},Ti_x)_3O_4$ nanoparticles. While the increase in temperature (ΔT) under 150 kHz RF signal reached up to 22°C in 10 minutes for SiO_2 coated $(Fe_{0.97},Ti_{0.03})_3O_4$ nanoparticles, which was very close value of uncoated Fe_3O_4 nanoparticles.

Keywords: oxide semiconductor, point defects, Neel relaxation, magnetic hypertermia, superparamagnetic nanoparticles

PACS: 75.50.Gg; 87.50.C-; 87.85.Rs; 87.19.Pp

***e-mail of corresponding author:** musamutlucan@gmail.com, **musa.can@istanbul.edu.tr**

Phone #: +090 (533) 929 0718

fax #: 090 (216) 483 9550

Introduction

Magnetite (Fe_3O_4) has an inverse spinel cubic structure with Fd-3m space group. The inverse spinel structure was form from [Fe3+] and [Fe2+] ions in tetrahedral and octahedral sites. Tetrahedral sites are occupied by 8 Fe3+ ions and octahedral sites are equally occupied by Fe2+ and Fe3+ ions co-ordinated with 32 oxygen atoms [Can, 2010; Can, 2006]. The ferrimagnetic properties were governed by the coupling of cations spins in octahedral and tetrahedral sites [Can, 2010; Can, 2006]. The properties, such as low toxicity, suitable magnetic properties and easily fabrication, make the ferrite particles suitable for hyperthermia usage [Fortin, 2008].

The magneto-heating processes is mainly associated with superparmagnetic particle size, particles interactions and homogenly distributed magnetic particles [Deatsch, 2014]. The magnetic relaxation is usually the dominant mechanism in magnetic hyperthermia. The magneto heating originating from two basic mechanisms, which govern the magnetization relaxation of magnetic nanoparticles. The internal magnetization relaxation and the rotational diffusion of whole magnetic nanoparticles are defined Néel relaxation and Brownian relaxation, respectivley

[Ilg, 2020]. The mechanism of magneto-heating is expected to be mainly depended on both mechanisms of Neel relaxation and Brownian relaxation [Celik, 2014; Ilg, 2020]. Both relaxations cause an increase in temperature, however for hypertermia applications Neel Relaxation has specific advantages, especially high specific absorption rate (SAR) value, according to the Brownain relaxation due to highly dependent on viscosity of surronded enviourment of particles [Fortin, 2008]. SAR value can be defined by absorbed/converted magnetic energy into thermal energy [Fortin, 2008]. Brownian relaxation is mainly effective for magnetic nanoparticles suspended in a viscous liquid, which permit the nanoparticles rotate freely [Ilg, 2020]. On the other hand, Neel relaxation occurs by Eddy currents on the particle surface [Hergt, 2009].

The Neel relaxation is dominant in superparamagnetic state due to low magnetic anisotropy [Hergt, 2009], and the increase of anisotropy make Brownian relaxation be dominant on magnetic heating mechanism [Deatsch, 2014]. The experiments, performed in solution, cell culture or in vivo, assign different factors affect the relaxation mechanisms and inhibit the mechanical rotations such as the different viscosities of the media, the nanoparticles agglomeration inside different cell or the nanoparticles fixation on cell membranes (or extracellular tissue) [Fabris, 2019]. The magneto heating mechanism without mechanical rotation will be independent from Brownian relaxation.

In our study, we expect that heating performance of individual, non-interacting and monodisperse particles have high SAR value due to be dominancy of Neel relaxation for highly viscose enviourments. According to our target we sythesize superparamagnetic Fe_3O_4 nanoparticles to make Neel relaxation maximum. Furthermore, Fe_3O_4 nanoparticles doped with Ti atoms in order to increase the numbers of free electrons, which improve the Eddy currents

enhancing the heating ability of nanoparticles. In addition, some times the heating mechanism of Fe_3O_4 nanoparticles can not be enough for cancer treatments and need to be surface modifications. The study also include to understand the SiO_2 coating impact on heating performance of $(Fe_{1-x},Ti_x)_3O_4$ nanoparticles. $(Fe_{1-x},Ti_x)_3O_4$ nanoparticles will be modified suitable for loading anticancer drugs and heating under both excitations, RF magnetic field and UV radiation, that utilize the magnetic nanoparticles useful at clinical hyperthermia applications in future studies.

Experimental

The magnetite nanoparticles were prepared via co-precipitation method. Ferrous chloride tetrahydrate and ferric chloride were used as iron precursors containing different valance states. On the other hand, Tetrtaisopropil Ortotinatate (TIPO) was used as Titanium source. Natrium Hydroxide 25%wt NaOH and hydrochloric acid (HCl) in water were employed as the precipitating agents. In order to prohibit to accumulation of magnetic nanoparticles, the nanoparticles were coated by Oleic acid at the end of procedure. Ethanol and DI water were used to remove excessive coating agent. The schematic diagram of procedure was demonstrated in figure 1. The synthesis was performed on magnetic stirrer at 90 ^oC. Firstly, ferrous and ferric chloride iron salts were dissolved in water with HCl under Argon gas flow. After half an hour, TIPO and NaOH were dropped to the solution. Oleic acid was added to the solution as a last step.

The coated nanoparticles were washed with DI water and ethanol to remove chloride ions and excessive coating materials. Furthermore, the same procedure was performed for synthesis of the pure magnetite nanoparticles.

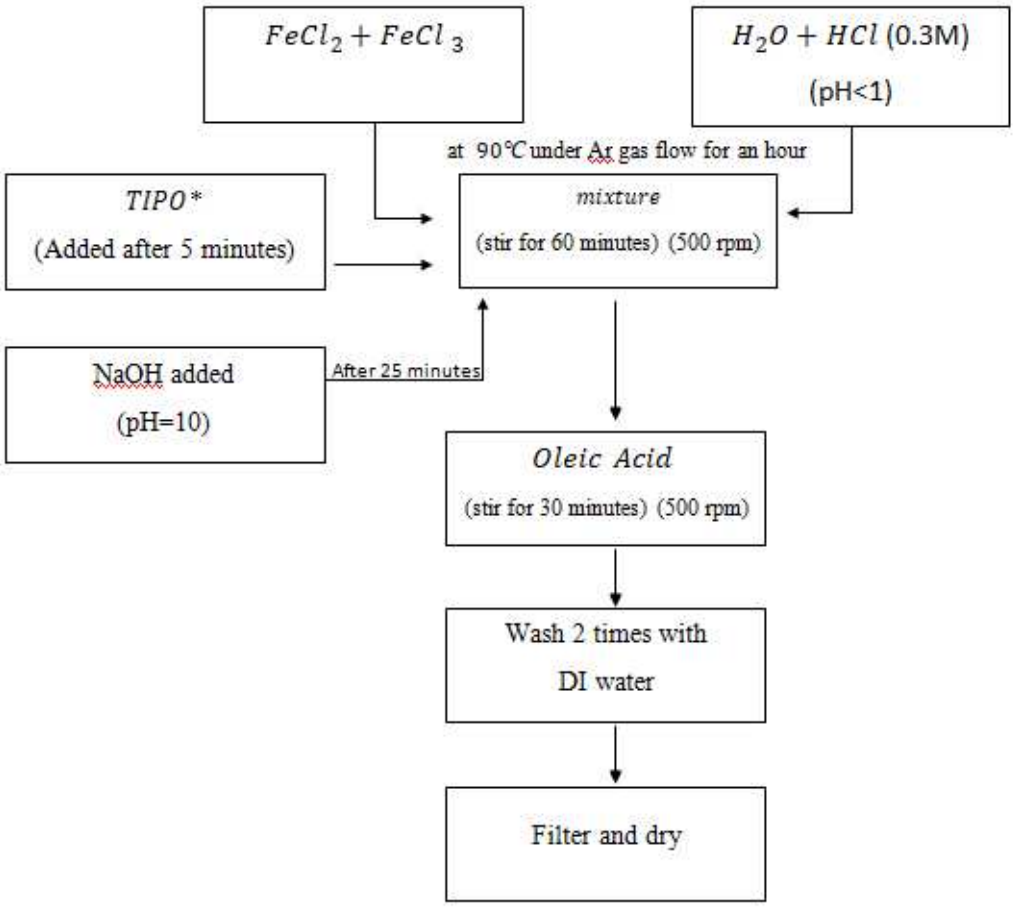

Figure 1. The schematic diagram of synthesis procedure of pure and Ti doped magnetite

The nanoparticles were also coated with SiO_2 by base-catalyzed silica formation from tetraethylorthosilicate (TEOS) in a water-in-oil microemulsion technique, which mentioned in previous study [Coskun, 2012]. The resulting mixture was vigorously stirred for more than 24 h.

The crystal structure of the samples was characterized by powder X-ray diffraction (XRD), using CoKα radiation. The morphologies of the nanoparticles and the shell thicknesses of the coated nanoparticles were characterized using a JEOL JEM-2010F high resolution transmission electron microscope (HRTEM). The dc magnetization (σ (H)) measurements were performed at 300 K

temperatures in the field range of ± 2 T. Magneto-thermal characterization were taken by a home-made setup constructed using the equipment with a frequency of 150 kHz (power generator, thermometer, etc.).

Result and Discussions:

The structural analysis were performed employing XRD patterns for both structures SiO_2 uncoated and coated particles as shown in figure 2a and figure 2b, respectively. The patterns were in an agreement with Fe_3O_4 diffraction pattern shown in ICDD card (PDF# 74-0748). No contamination or unexpected phase such as TiO_2 based structures, was detected on the XRD patterns. As seen on figure 2b, even though the high background intensity, originating from the amorphous phase of SiO_2, the Fe_3O_4 patterns were distinctly distinguished at each XRD pattern.

Ti elements or compounds were not detected on the patterns, which indicated the replacement of Ti atoms inside of Fe_3O_4 lattice. The ionic radius of Ti^{4+} is approximately 0.61Å, which is close to ionic radius of Fe^{3+} (0.64 Å). Thus, Ti^{4+} ions are expected to replace on octahedral lattice sites instead of Fe^{3+} ions and coupled with Fe^{2+} ions. Due to charge neutrality, a Ti^{4+} ion replacement in octahedral site gives rise to change valence state of Fe^{3+} ion to Fe^{2+} ion as shown in chemical equation of (1) [Walz, 1997].

$$2Fe^{3+} \rightarrow Ti^{4+} + Fe^{2+} \quad (1)$$

Increasing Ti^{4+} substitution ($0.01 \leq x \leq 0.025$) cause to be form of $Fe^{2+}{}_A(Fe^{2+}\ Ti^{4+})_BO4$ (A: tetrahedral side, B: octahedral side), which inhibits the hopping mechanism between iron ionic states and cause to increase in magnetic anisotropy as mentioned in literature [Walz, 1997; Kakol,

1993]. Excessive Ti^{4+} substitution ($x \geq 0.025$) cause to form different vacancies, readily jumping Fe^{2+} ions [Walz, 1997].

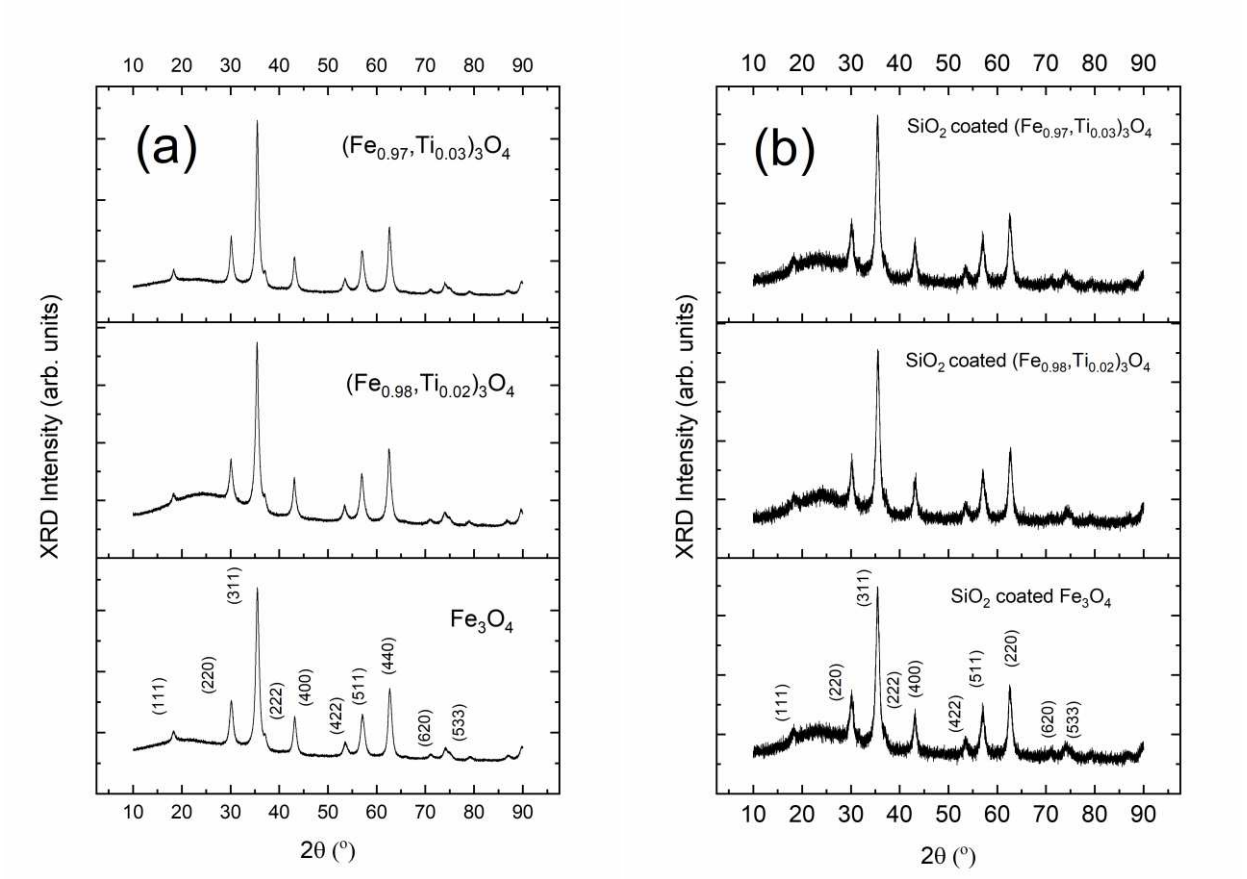

Figure 2. The xrd patterns of (a) Ti doped magnetite and (b) SiO_2 coated Ti doped magnetite

After understanding the crystal structure, the particle sizes were obtained employing TEM micrographs. TEM figures proved that the particles were not agglomerated due to covering with oleic acid matrix as seen on figure 3. TEM figures assigned homogeny distributed particles and the size frequencies of particles were calculated by subprogram of Image-J. Particles with high differences in particle size were selected in the calculations. As shown on figure 4, the particles size distributions, calculated via ImageJ, were found as 10.3±0.6 nm and 18.7±0.5 nm for

uncoated and coated $(Fe_{0.97},Ti_{0.03})_3O_4$, respectively. The particles size distribution indicated that the particles were in superparamagnetic regions.

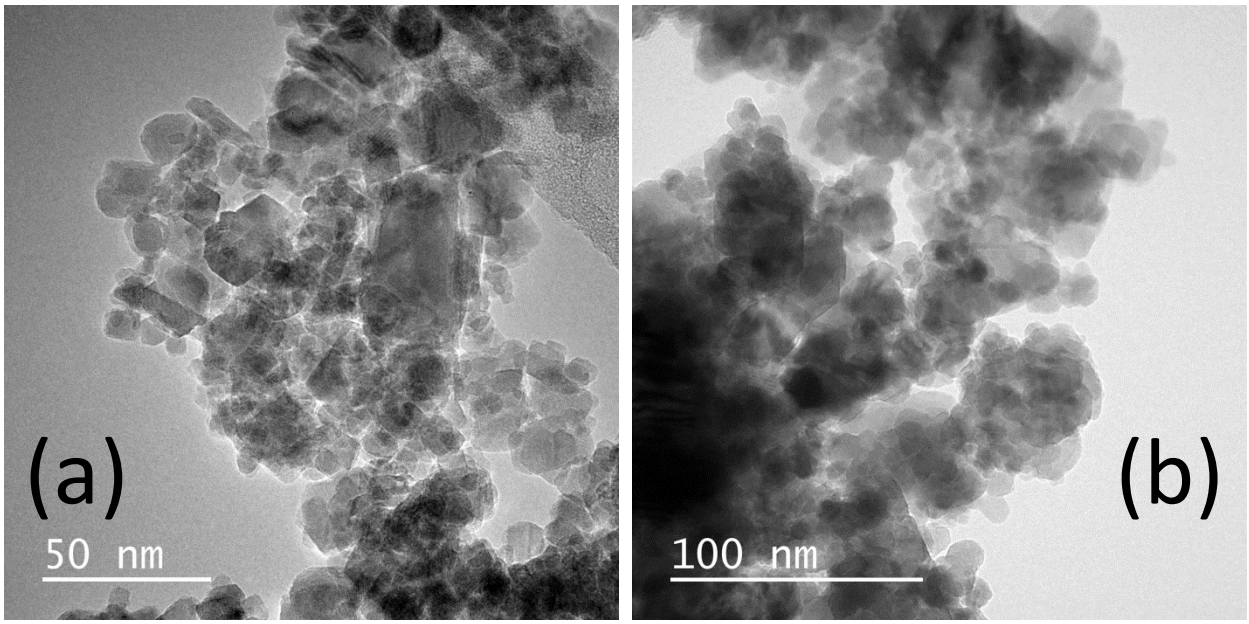

Figure 3. TEM micrographs of (a) uncoated and (b) coated $(Fe_{0.97},Ti_{0.03})_3O_4$ nanoparticles.

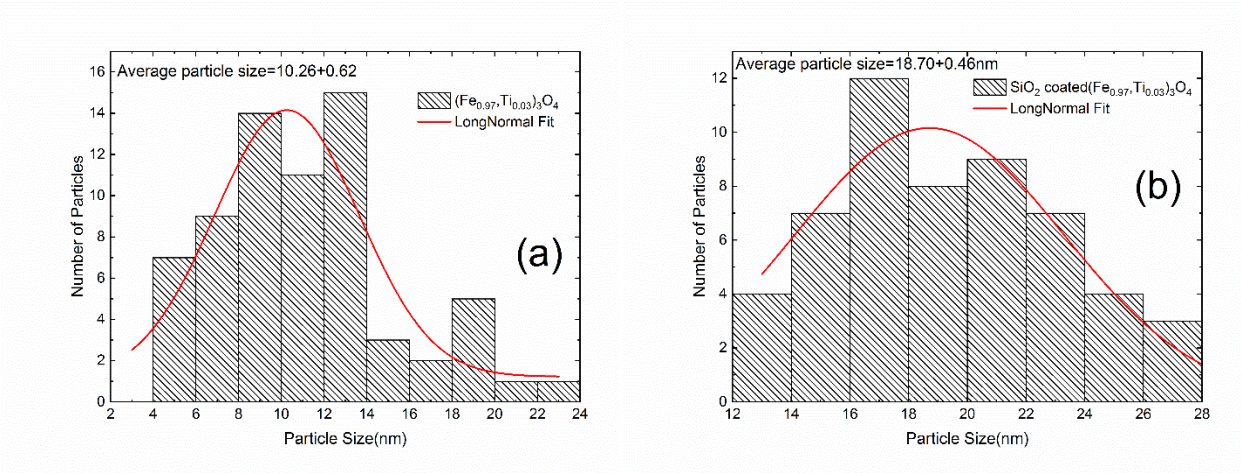

Figure 4. Calculated size distributions of (a) uncoated and (b) coated $(Fe_{0.97},Ti_{0.03})_3O_4$ nanoparticles via ImageJ subprogramme.

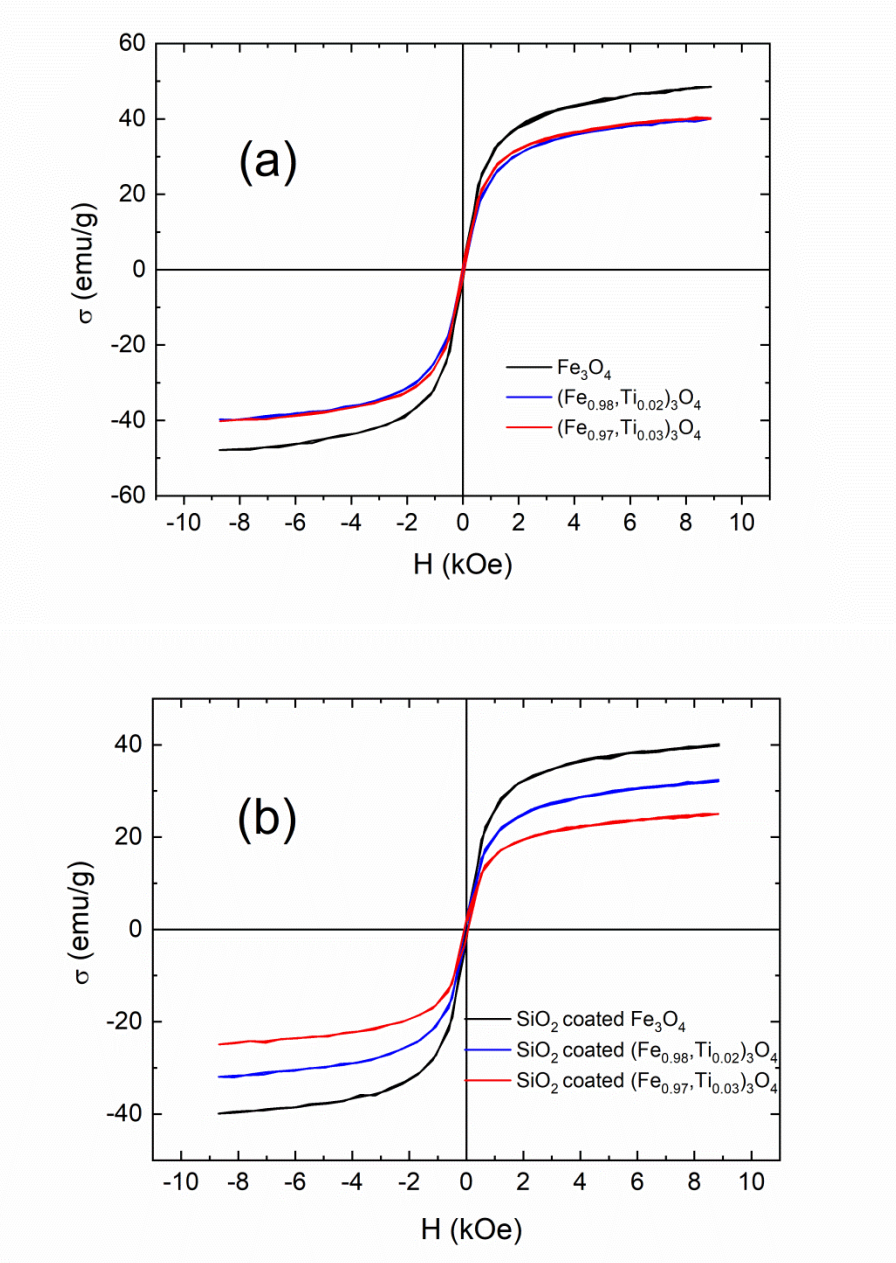

Figure 5. The magnetization measurements of (a) uncoated and, (b) SiO_2 coated pure and Ti doped magnetite

The magnetization (σ (H)) measurements at room temperature were illustrated in the figure 5 for both samples uncoated and coated $(Fe_{1-x},Ti_x)_3O_4$. As seen from the figure, the zero remanent magnetization assign the overcoming thermal energy to the magnetic anisotropy energy barrier at

all samples. The only difference in magnetization curves was the decrease in magnetization by Ti doping amount in magnetite lattice.

On the other hand, overcoming thermal energy to magnetic energy at the room temperature indicated that synthesized nanoparticles were in superparamagnetic region. Because of being the particles in superparamagnetic state size, the common properties of nano particles obey the Neel type and thus, intra particle magnetic moments are dominant in magneto heat effect in these particles.

The magnetic heating performance of particles were illustrated in figure 6. The magneto heating measurements of uncoated and coated nanoparticles were taken by mixing nanoparticles as magnetofluids in 1 ml ethanol media. Instead of using magneto heating, the physical quantity can be determined by the specific absorption rate (SAR) defined as the heat released from colloidal magnetic nanoparticles in unit time by equation (3) [Rosensweig, 2002].

$$SAR = \frac{Q}{\Delta t \, m_{mag}} \tag{3}$$

where $Q = mc\Delta T, m_{mag}$is the mass of magnetic particle, c is the specific heat of the colloid (only ethanol is taken into account, the contribution of MNPs, oleic acid and SiO_2 to the specific heat are neglected). The calculations were performed for the heat capacity and the density of ethanol 2.57 kJ/(kgK), 0.789 g/mL respectively.

Table 1. SAR values of $(Fe_{1-x},Ti_x)_3O_4$ (x=0.00, 0.02 and 0.03) nanoparticles

Nanoparticles	**SAR (W/g)**
Fe_3O_4	155
SiO_2 coated Fe_3O_4	104
x=0.02	70
x=0.03	3
x=0.02 (SiO_2 coated)	34
x=0.03 (SiO_2 coated)	116

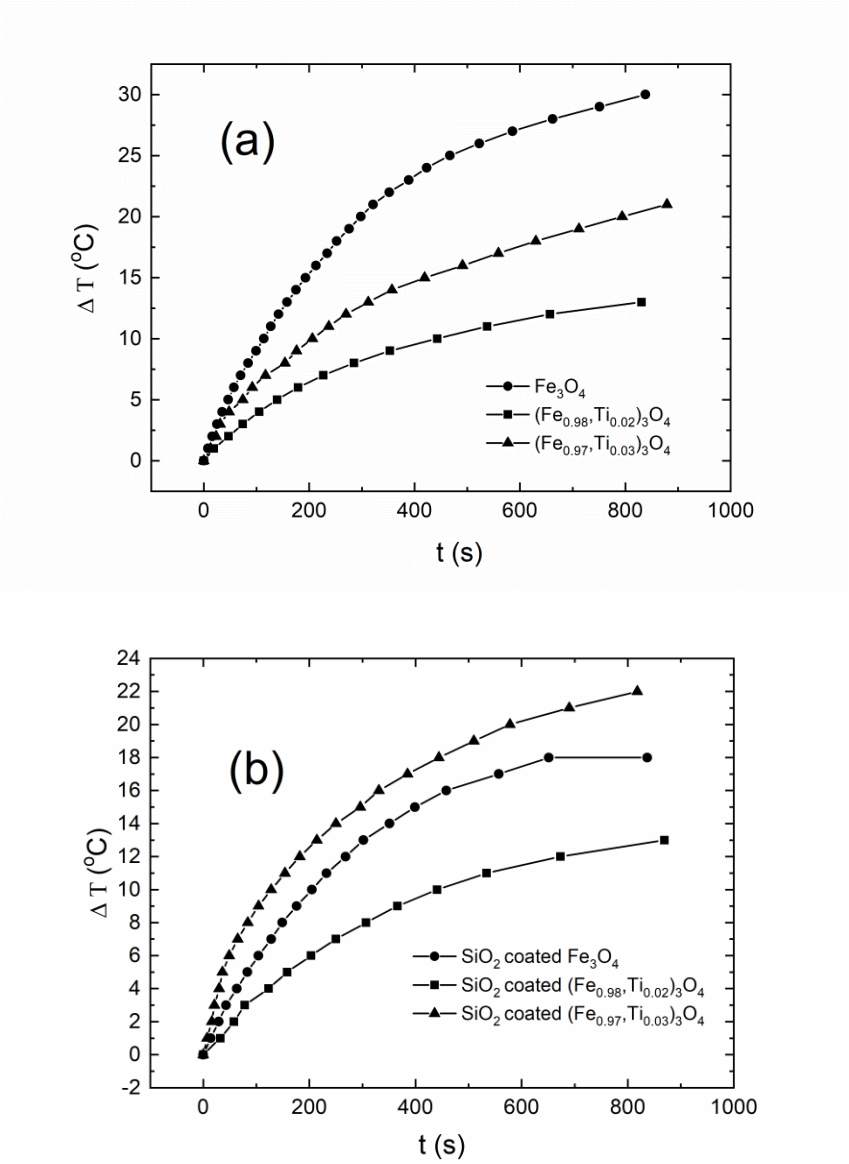

Figure 6. The magnetic heating performance of (a) uncoated and, (b) SiO_2 coated pure and Ti doped Fe_3O_4.

Calculated SAR values were illustrated in Table 1. As understood from table 1, coating with SiO_2 cause a specific decrease in SAR values of $(Fe_{1-x},Ti_x)_3O_4$ nanoparticles. However, Ti^{4+} ions amount induces an increase in SAR value, which getting closer to the value of pure Fe_3O_4 nanoparticles.

Conclusion

In the study, homogeny size distributed $(Fe_{1-x},Ti_x)_3O_4$ ferrite nanoparticles in oleic acid and at SiO_2 matrix were synthesized via chemical route. The particles behaved as superparamagnetic at room temperature. We expect that heating performance of individual, non-interacting and monodisperse particles have high SAR value due to be dominancy of Neel relaxation for highly viscose environments. According to our target we sythesize superparamagnetic Fe_3O_4 nanoparticles to make Neel relaxation maximum. In addition $(Fe_{1-x},Ti_x)_3O_4$ nanoparticles were coated with SiO_2 to decrease the interparticle interaction and to get rid of Brownian relaxation mechanism.

Heat production mechanism under the ac magnetic field is determined by applying approximately 13 kA/m field intensity and 150 kHz frequency under biological limits of 5×10^9 A/(m.sec). The heating mechanism of SiO_2 coated Ti doped Fe_3O_4 nanoparticles were only correlated with Ti atoms amount in lattice. For 4 mol% Ti doping, the heating performans was very low according to the pure Fe_3O_4 due to Ti^{4+} - Fe^{2+} coupling at octahedral side. The increase in amount of Ti^{4+} ions in lattice cause an increase in SAR value of SiO_2 coated $(Fe_{0.97},Ti_{0.03})_3O_4$ nanoparticles ($\Delta T=22^oC$ in 10 minutes), while decreasing for uncoated nanoparticles. The heating performance of $(Fe_{0.97},Ti_{0.03})_3O_4$ nanoparticles coated with SiO_2 was almost close to the heating performance of pure magnetite.

Acknowledgement

This work was also supported by Scientific Research Projects Coordination Unit of Istanbul University with project number FBG-2018-28289.

References

[Can, 2011] Can, M. M., Coşkun, M., Fırat, T., Domain state–dependent magnetic formation of Fe_3O_4 nanoparticles analyzed via magnetic resonance, Journal of Nanoparticle Research 13 (2011) 10, 5497

[Can, 2006] Can, M. M., Ozcan, S., Fırat, T., Magnetic behaviour of iron nanoparticles passivated by oxidation, Physica Status Solidi c, 3 (2006) 5, 1271-1278

[Celik, 2014] Çelik, Ö., Can, M. M., Firat, T., Size dependent heating ability of $CoFe_2O_4$ nanoparticles in AC magnetic field for magnetic nanofluid hyperthermia, Journal of Nanoparticle Research, 16 (2014) 3, 2321

[Coskun, 2012] Coskun, M., Can, M. M., Duyar-Coskun, Ö., Korkmaz, M., Fırat, T., Surface anisotropy change of $CoFe_2O_4$ nanoparticles depending on thickness of coated SiO_2 shell, Journal of Nanoparticle Research, 14 (2012) 10, 1197

[Deatsch, 2014] Deatsch, A. E., Evans, B. A., Heating efficiency in magnetic nanoparticle hyperthermia, Journal of Magnetism and Magnetic Materials, 354 (2014), 163-172

[Fabris, 2019] Fabris, F., Lima, E. Jr., De Biasi, E., Troiani, H. E., Mansilla, M. V., Torres, T. E., Pacheco, R. F., Ibarra, M. R., Goya, G. F., Zysler, R. D., Winkler, E. L. Controlling the dominant magnetic relaxation mechanisms for magnetic hyperthermia in bimagnetic core–shell nanoparticles, Nanoscale, 2019, 11, 3164-3172

[Fortin, 2008] Fortin, J.-P., Gazeau, F., Wilhelm, C., Intracellular heating of living cells through Neel relaxationof magnetic nanoparticles, Eur Biophys J, 37 (2008), 223–228

[Ilg, 2020] Ilg, P., Kröger, M., Dynamics of interacting magnetic nanoparticles: effective behavior from competition between Brownian and Néel relaxation, Phys. Chem. Chem. Phys., 22 (2020), 22244-22259

[Hergt, 2009] Hergt, R., Dutz, S., Zeisberger, M., Validity limits of the Néel relaxation model of magnetic nanoparticles for hyperthermia, Nanotechnology 21 (2009), 015706

[Kakol, 1994] Z. Kakol, J. Sabol, J. Stickler, A. Kozfowski, J. M. Honig, Influence of titanium doping on the magneto crystalline anisotropy of magnetite, Physical Review B, 49 (1994) 18, 12767-12772

[Rosensweig, 2002] R. E. Rosensweig, Heating Magnetic Fluid with Alternating Magnetic Field, J Magn. Magn. Mater., 252 (2002) 370-374.

[Walz, 1997] F. Walz, L. Torres, K. Bendimya, C.de Francisco, H. Kronmuller, Analysis of Magnetic After-Effect Spectrain Titanium-Doped Magnetite, phys. stat. sol. (a), 164 (1997), 805

Figures

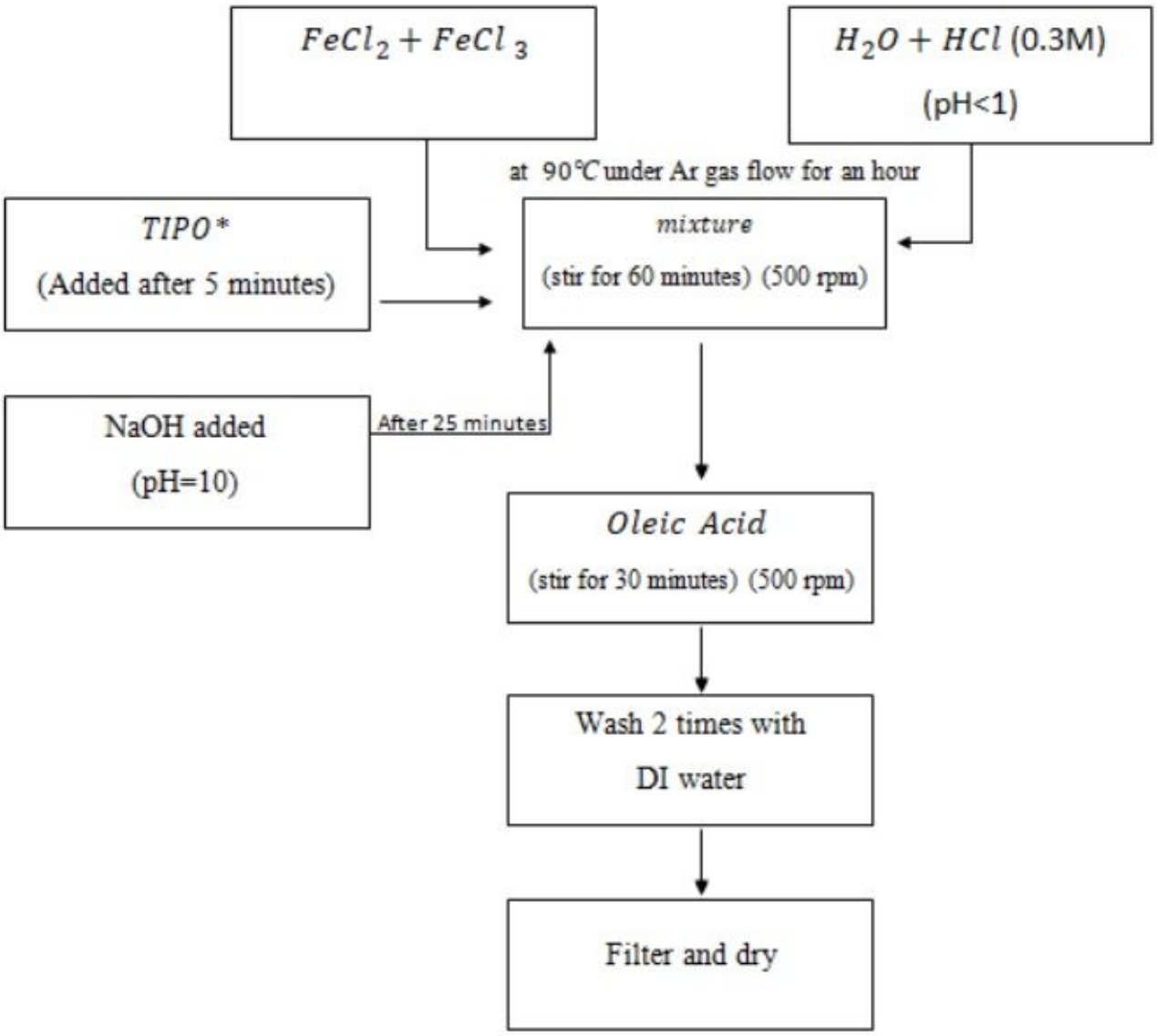

Figure 1

The schematic diagram of synthesis procedure of pure and Ti doped magnetite

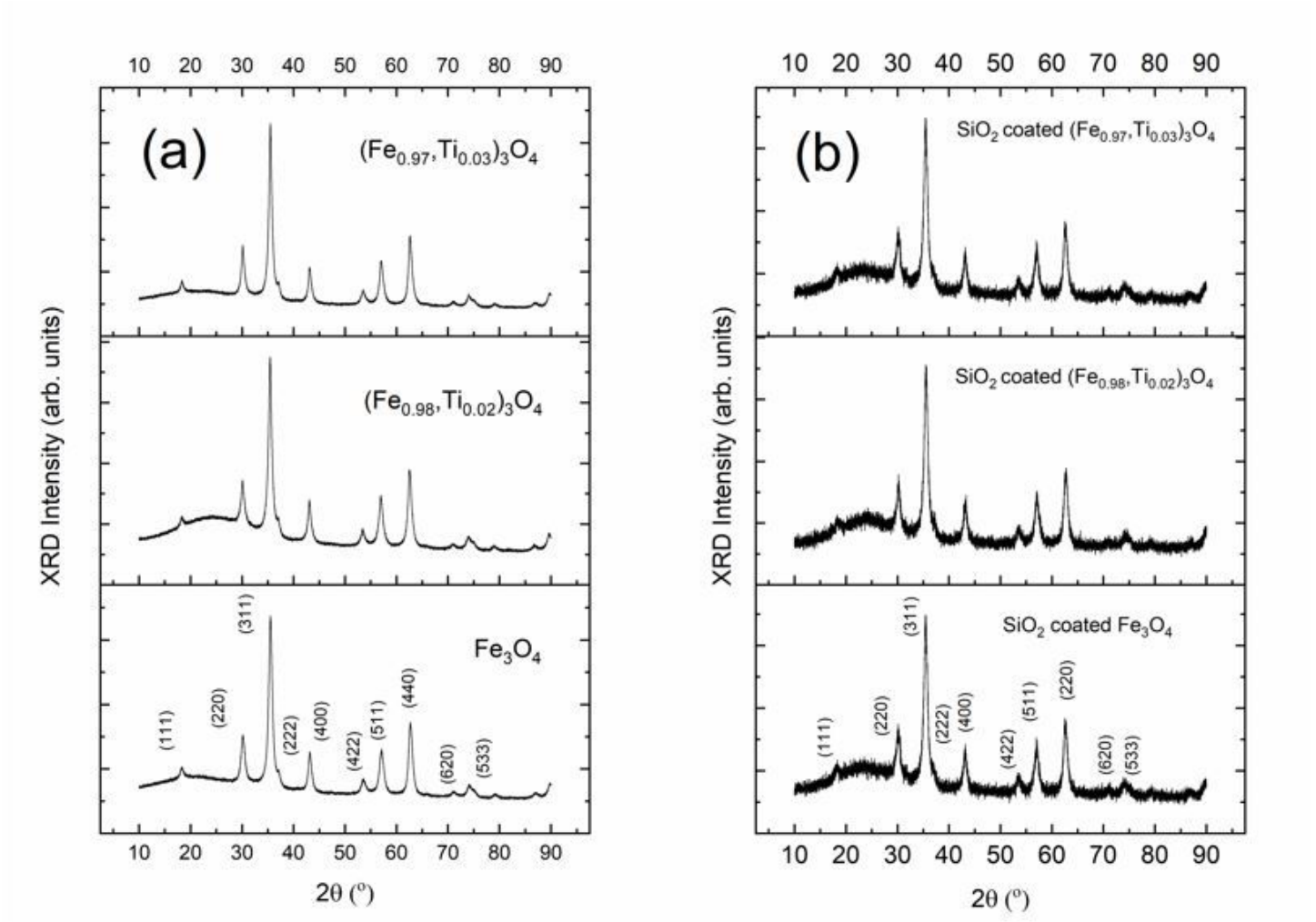

Figure 2

The xrd patterns of (a) Ti doped magnetite and (b) SiO2 coated Ti doped magnetite

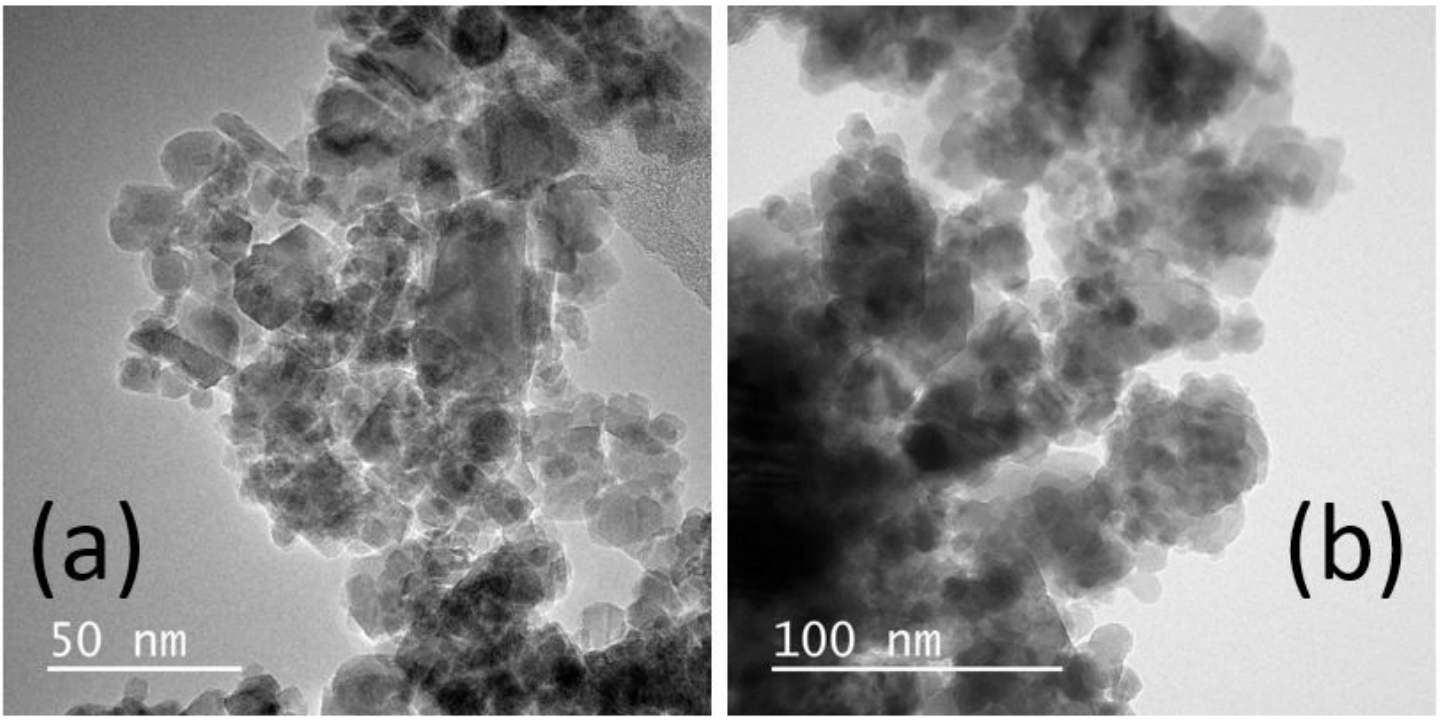

Figure 3

TEM micrographs of (a) uncoated and (b) coated (Fe0.97,Ti0.03)3O4 nanoparticles.

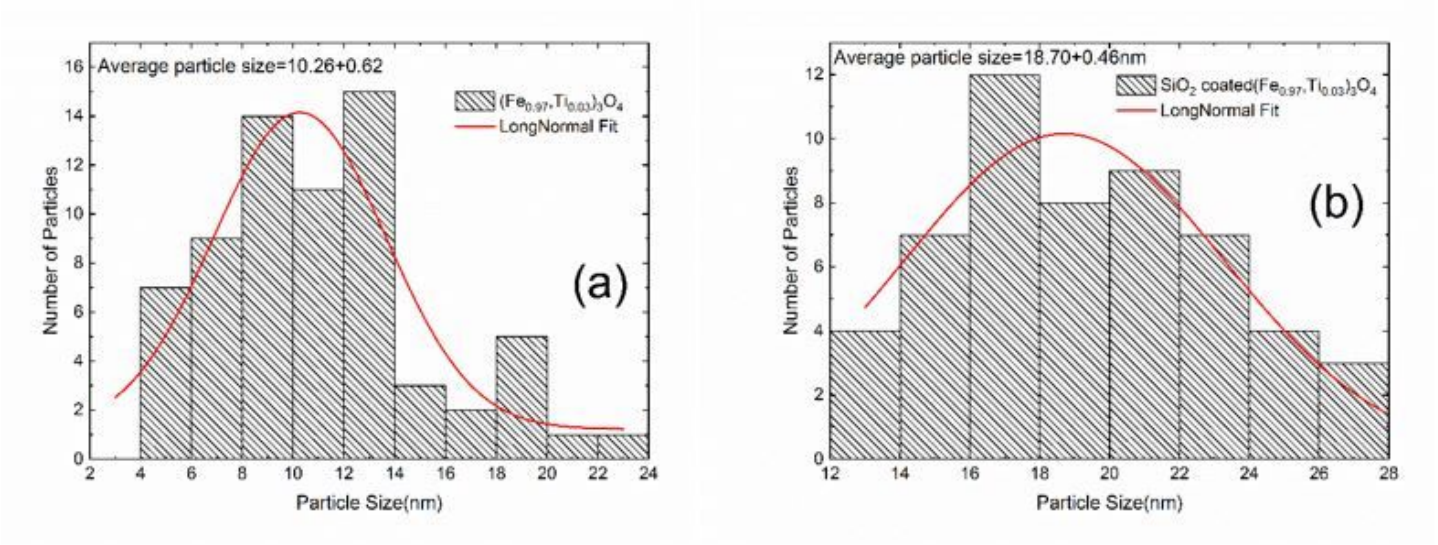

Figure 4

Calculated size distributions of (a) uncoated and (b) coated (Fe0.97,Ti0.03)3O4 nanoparticles via ImageJ subprogramme.

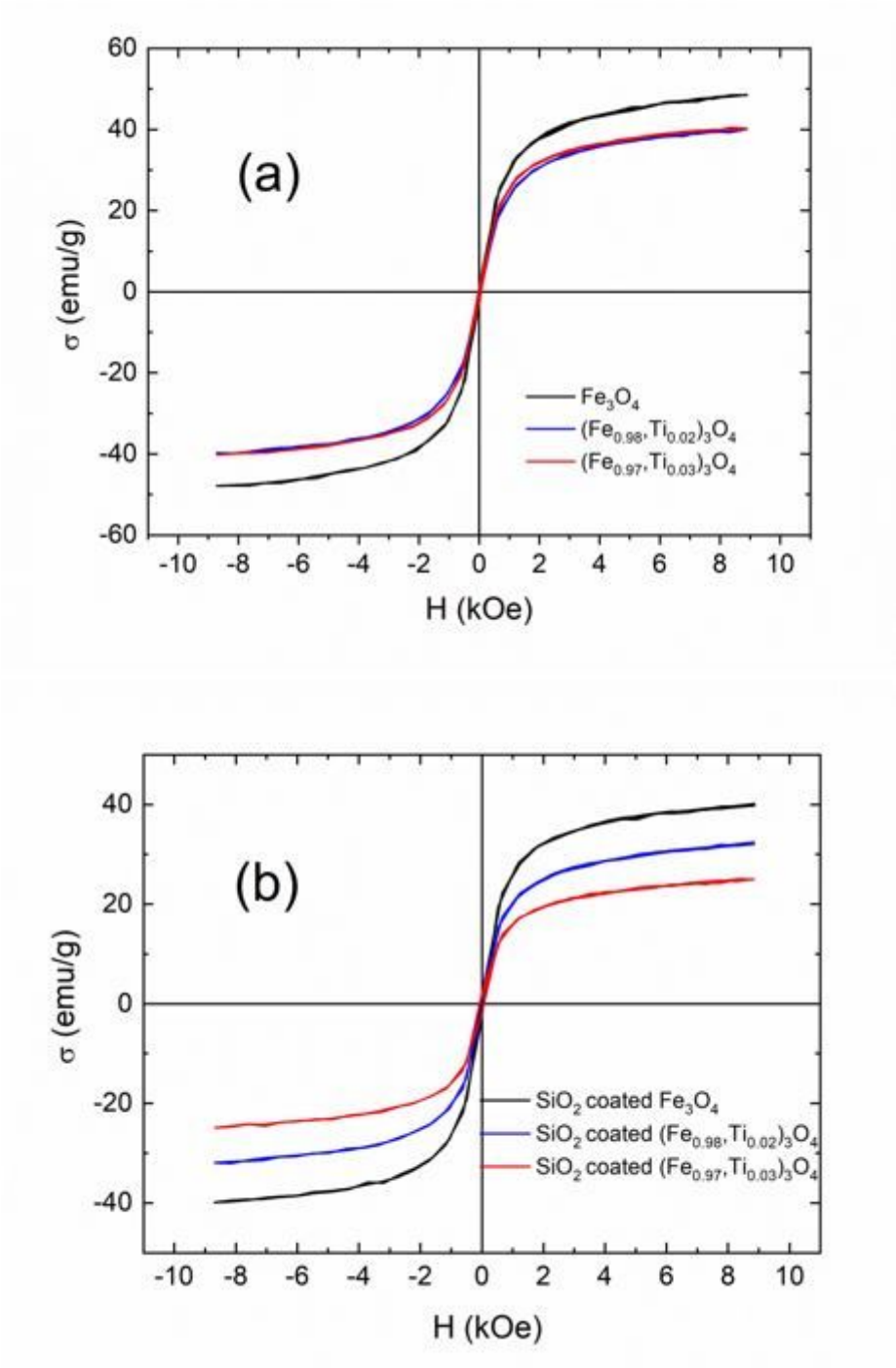

Figure 5

The magnetization measurements of (a) uncoated and, (b) SiO2 coated pure and Ti doped magnetite

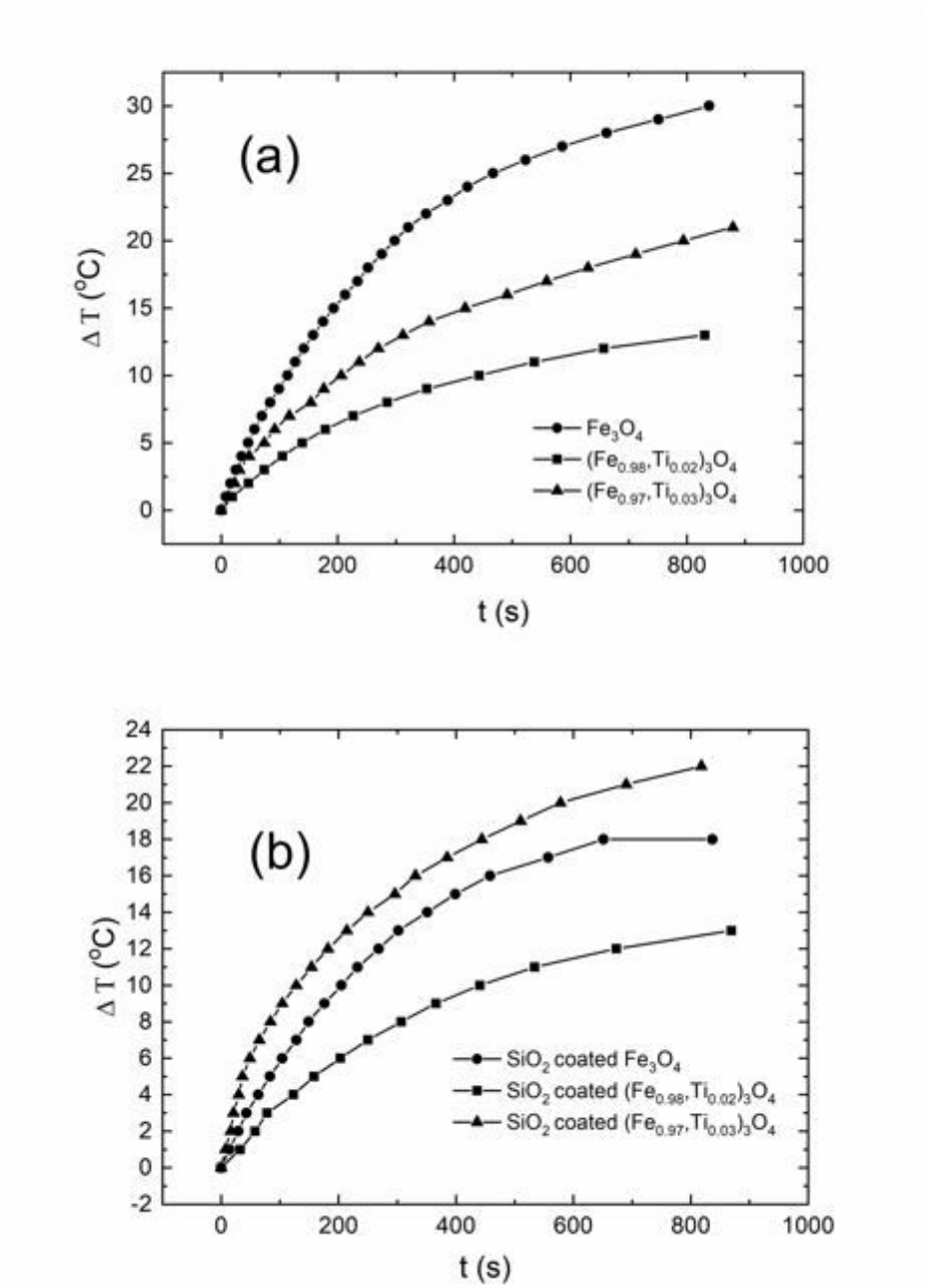

Figure 6

The magnetic heating performance of (a) uncoated and, (b) SiO2 coated pure and Ti doped Fe3O4.